

Limit behaviour of Eringen's two-phase elastic beams

Preprint of the article published in
European Journal of Mechanics - A/Solids
89, August–October 2021, 104315

Marzia Sara Vaccaro,
Francesco Paolo Pinnola,
Francesco Marotti de Sciarra,
Raffaele Barretta

<https://doi.org/10.1016/j.euromechsol.2021.104315>

© 2021. This manuscript version is made available under the CC-BY-NC-ND 4.0 license <http://creativecommons.org/licenses/by-nc-nd/4.0/>

Limit behaviour of Eringen's two-phase elastic beams

Marzia Sara Vaccaro, Francesco Paolo Pinnola, Francesco Marotti de Sciarra, Raffaele Barretta^a

^a *Department of Structures for Engineering and Architecture,
University of Naples Federico II, via Claudio 21, 80125 - Naples, Italy
e-mail: rabarret@unina.it*

Abstract

In this paper, the bending behaviour of small-scale Bernoulli-Euler beams is investigated by Eringen's two-phase local/nonlocal theory of elasticity. Bending moments are expressed in terms of elastic curvatures by a convex combination of local and nonlocal contributions, that is a combination with non-negative scalar coefficients summing to unity. The nonlocal contribution is the convolution integral of the elastic curvature field with a suitable averaging kernel characterized by a scale parameter. The relevant structural problem, well-posed for non-vanishing local phases, is preliminarily formulated and exact elastic solutions of some simple beam problems are recalled. Limit behaviours of the obtained elastic solutions, analytically evaluated, studied and diagrammed, do not fulfill equilibrium requirements and kinematic boundary conditions. Accordingly, unlike alleged claims in literature, such asymptotic fields cannot be assumed as solutions of the purely nonlocal theory of beam elasticity. This conclusion agrees with the known result which the elastic equilibrium problem of beams of engineering interest formulated by Eringen's purely nonlocal theory admits no solution.

Key words: Purely nonlocal elasticity, Local/nonlocal mixture, Nanobeams, Well-posedness, Constitutive boundary conditions

1. Introduction

Over the past decades, growing interest in nanotechnological applications has required a deep knowledge of mechanical behavior of micro- and nano-structures conceived as basic components of smaller and smaller electro-mechanical devices. Among the wide variety of micro/nano-electro-mechanical

systems there are biosensors (Soukarié et al., 2020), actuators (Lu et al., 2019), resonators (Chorsi and Chorsi, 2018), DNA switches (Chao et al., 2020), porous structures (Jankowski et al., 2020; Malikan et al., 2020b), valves/pumps (Banejad et al., 2020), advanced and composite structures (Sedighi et al., 2017; Żur et al., 2020), energy harvesters (Ghayesh and Farokhi, 2020).

Micro/nano-structures exhibit technically significant size effects which therefore have to be taken into account to accurately model and design new-generation small-scale devices (Ghayesh and Farajpour, 2019). To this end, nonlocal continuum mechanics (Polizzotto, 2001, 2002; Bažant and Jirásek, 2002; Borino et al., 2003) has been conveniently exploited by the scientific community to simulate complex scale phenomena in place of atomistic approaches which are computationally expensive.

One of the first theories of nonlocal elasticity is the strain-driven model introduced by Eringen (1983) in the wake of seminal contributions by Rogula (1965); Kröner et al. (1967); Rogula (1982). According to the strain-driven model, the nonlocal stress field is the convolution integral between elastic strain and an averaging kernel depending on a characteristic length. Originally exploited by Eringen to deal with screw dislocations and surface waves, when applied to structural problems involving bounded domains, Eringen's strain-driven model leads to ill-posed structural problems due to incompatibility between nonlocal and equilibrium requirements (Romano et al., 2017a).

An effective strategy to get well-posed problems consists in formulating a new nonlocal model in which the roles of stresses and strains are swapped (Romano et al., 2017b). The stress-driven nonlocal approach has been successfully applied to a wide range of problems of nanotechnological interest (see e.g. Barretta et al., 2018b; Roghani, 2020; Zhang, 2020; Barretta et al., 2018c; Pinnola, 2020; Oskouie et al., 2018; Barretta et al., 2019).

Another possible strategy to overcome ill-posedness of strain-driven model consists in formulating a two-phase local/nonlocal model, first introduced in (Eringen, 1972, 1987) and recently applied in (Pisano and Fuschi, 2003; Khodabakhshi and Reddy, 2015; Wang et al., 2016; Eptaimeros et al., 2016; Barretta et al., 2018a). In particular, the mixture strain-driven model is based on a convex combination of local and nonlocal phases by means of a mixture parameter, where the nonlocal phase is the Eringen's integral convolution. Based on two parameters, the two-phase theory is able to model a lot of structural problems. However, ill-posedness is eliminated only for positive mixture parameters (Romano et al., 2017b).

Indeed, for vanishing local phases, Eringen’s purely nonlocal strain-driven law is recovered, and hence inconsistencies are expected to occur for structural nonlocal solutions of the limiting elastic equilibrium problem.

In this regard, inaccurate conclusions on the matter are still present in current literature (see e.g. [Mikhasev and Nobili, 2020](#); [Mikhasev, 2021](#)) by improperly defining limiting cases of free vibration problems as solutions of elastodynamic problems based on purely nonlocal strain-driven continuum model which admits no solution ([Romano et al., 2017a](#); [Fernández-Sáez and Zaera, 2017](#); [Fathi and Ghassemi, 2017](#); [Vila et al., 2017](#); [Zhang, 2017](#); [Zhu and Li, 2017](#); [Karami et al., 2018](#); [Barretta et al., 2018b](#); [Pisano et al., 2021](#)).

Inconsistencies of limiting solutions of structural problems based on Eringen’s two-phase theory will be definitely provided in the present research. The plan is the following. The two-phase integral model for slender beams is recalled in [Sec.2](#) and the equivalent differential problem is also provided. The purely nonlocal strain-driven law is then derived and discussed in [Sec.3](#). Exact structural solutions based on two-phase theory are given in [Sec.4](#) for simple applicative cases. Analytical limiting solutions, presented in [Sec.5](#), are shown to be in contrast with equilibrium and kinematic boundary conditions. Consequently, such fields cannot be assumed as solutions of structural problems formulated according to Eringen’s purely nonlocal strain-driven model which is thus confirmed as inapplicable to nanocontinua of technical interest.

2. Two-phase local/nonlocal theory for elastic beams

Let us consider a slender straight beam under flexure of length L . Beam and bending axes are denoted by x and y respectively. According to Bernoulli-Euler theory, the total curvature field $\chi : [0, L] \mapsto \mathfrak{R}$ associated with the transverse displacement field $v : [0, L] \mapsto \mathfrak{R}$ is expressed by¹

$$\chi = \partial_x^2 v = \chi^{el} + \chi^{nel} \quad (1)$$

with χ^{el} elastic curvature and χ^{nel} all other non-elastic curvature fields. Stress fields are described by bending moments $M : [0, L] \mapsto \mathfrak{R}$ which have to fulfill the differential equation of equilibrium

$$\partial_x^2 M = q \quad (2)$$

¹The symbol ∂_x^n denotes n -times differentiation along the beam axis x .

with $q : [0, L] \mapsto \Re$ transversely distributed loading.

According to the two-phase elasticity model (Eringen, 1972), the bending moment M is convex combination of the source field $s := K\chi^{el}$ and of the convolution between the source s and a suitable averaging kernel ϕ_c

$$M(x) = \alpha s(x) + (1 - \alpha) \int_0^L \phi_c(x, \xi) s(\xi) d\xi \quad (3)$$

where K is the local elastic bending stiffness, i.e. second moment of the field of Euler-Young elastic moduli E on beam cross section.

The relation in Eq.(3) is a Fredholm integral equation of the second kind (Tricomi, 1957; Polyanin and Manzhirov, 2008) in the unknown source field s , with $0 \leq \alpha \leq 1$ mixture parameter and $c > 0$ nonlocal scale parameter.

The purely nonlocal law $M(x) = \int_0^L \phi_c(x, \xi) K\chi^{el}(\xi) d\xi$ is got by setting $\alpha = 0$, while for $\alpha = 1$ the purely local relation $M = K\chi^{el}$ is recovered.

The averaging kernel is assumed to be the bi-exponential function

$$\phi_c(x) = \frac{1}{2c} \exp\left(-\frac{|x|}{c}\right) \quad (4)$$

fulfilling symmetry, positivity and limit impulsivity (Eringen, 1983).

An equivalent differential formulation (Romano et al., 2017a) of the two-phase model Eq.(3) can be got by observing that the special kernel in Eq.(4) is the Green's function of the linear differential operator \mathcal{L}_x defined by

$$\mathcal{L}_x := 1 - c^2 \partial_x^2 \quad (5)$$

Now, rewriting Eq.(3) as follows

$$(M - \alpha K\chi^{el})(x) = (1 - \alpha) \int_0^L \phi_c(x, \xi) K\chi^{el}(\xi) d\xi \quad (6)$$

and applying the differential operator \mathcal{L}_x to Eq.(6), we get

$$\mathcal{L}_x(M - \alpha K\chi^{el})(x) = (1 - \alpha) K\chi^{el}(x) \quad (7)$$

which is the differential equation equivalent to the two-phase model in Eq.(3).

Indeed, denoting by δ the Dirac unit impulse, since $\mathcal{L}_x \phi_c(x, \xi) = \delta(x, \xi)$, we may write

$$\mathcal{L}_x(M - \alpha K \chi^{el})(x) = (1 - \alpha) \int_0^L \mathcal{L}_x \phi_c(x, \xi) K \chi^{el}(\xi) d\xi = (1 - \alpha) K \chi^{el}(x) \quad (8)$$

As proven in (Romano et al., 2017a), the special kernel in Eq.(4) satisfies the following homogeneous boundary conditions

$$\begin{cases} \mathcal{B}_0 \phi_c |_0 = 0 \\ \mathcal{B}_L \phi_c |_L = 0 \end{cases} \quad (9)$$

where $\mathcal{B}_0 := 1 - c \partial_x$ and $\mathcal{B}_L := 1 + c \partial_x$ are differential operators defined at the boundary. By applying \mathcal{B}_0 and \mathcal{B}_L to Eq.(6) we get

$$\begin{cases} \mathcal{B}_0(M - \alpha K \chi^{el}) |_0 = 0 \\ \mathcal{B}_L(M - \alpha K \chi^{el}) |_L = 0 \end{cases} \quad (10)$$

which are the constitutive boundary conditions associated with Eq.(7).

Finally, the equivalent differential problem in Eqs.(7)-(10) can be explicitly formulated as follows

$$\frac{M(x)}{c^2} - \partial_x^2 M(x) = \frac{(K \chi^{el})(x)}{c^2} - \alpha \partial_x^2 (K \chi^{el})(x) \quad (11)$$

$$\begin{cases} \partial_x M(0) - \frac{1}{c} M(0) = \alpha \left(\partial_x (K \chi^{el})(0) - \frac{(K \chi^{el})(0)}{c} \right) \\ \partial_x M(L) + \frac{1}{c} M(L) = \alpha \left(\partial_x (K \chi^{el})(L) + \frac{(K \chi^{el})(L)}{c} \right) \end{cases} \quad (12)$$

3. Limiting case: purely nonlocal elasticity

For vanishing mixture parameter $\alpha = 0$, the purely nonlocal elasticity model is recovered, that is

$$M(x) = \int_0^L \phi_c(x, \xi) (K\chi^{el})(\xi) d\xi \quad (13)$$

which is the Eringen's purely nonlocal strain-driven law.

Remark. For any value of $c > 0$, the integral convolution Eq.(13) admits a unique solution (or no solution) if and only if the following constitutive boundary conditions are satisfied by the bending field (Romano et al., 2017a)

$$\begin{cases} \partial_x M(0) - \frac{1}{c} M(0) = 0 \\ \partial_x M(L) + \frac{1}{c} M(L) = 0 \end{cases} \quad (14)$$

Fulfillment of Eq.(14) ensures that differential equation (Eq.(15)) provides the unique solution of the nonlocal problem (Romano et al., 2017a)

$$\frac{M(x)}{c^2} - \partial_x^2 M(x) = \frac{(K\chi^{el})(x)}{c^2} \quad (15)$$

As proven in (Romano et al., 2017a), constitutive boundary conditions Eqs.(14) are incompatible with equilibrium requirements, since they relate bending and shearing fields through the characteristic nonlocal length c . The two-phase model eliminates ill-posedness for $\alpha > 0$. Indeed, left-hand sides of Eq.(12) are known expressions (generally polynomial), unless of n integration constants, with n redundancy degree. Hence, the laws in Eq.(12) are non-homogeneous boundary conditions imposed on the elastic curvature and its first derivative and no incompatibility arises with kinematic boundary constraints since they act on displacement fields and its first derivatives. However, as $\alpha \rightarrow 0$ the two-phase strain-driven law will tend to an ill-posed theory and then inconsistencies of limiting solutions are expected to occur. Predicted singularities for $\alpha \rightarrow 0$ will be investigated in detail in the sequel.

4. Case-studies and exact structural solutions

This section provides exact closed-form solutions of the elastic equilibrium problem of inflected beams using Eringen's two-phase model Eqs.(11)-(12). The solution procedure is summarized as follows.

- **Step 1.** Solution of the differential equilibrium condition in Eq.(2) equipped with standard natural boundary conditions to get the bending moment as functions of n integration constants, with n standing for redundancy degree. For statically determinate beams, the equilibrated bending field is univocally determined by equilibrium requirements.
- **Step 2.** Inserting the obtained bending field M in the equivalent differential problem governed by Eqs.(11)-(12) to get the nonlocal elastic curvature field χ^{el} .
- **Step 3.** Detection of nonlocal displacement field v by solving Eq.(1) with prescription of $3 + n$ standard essential boundary conditions.

The solution procedure above is applied to solve the nonlocal elastostatic problems below. The non-elastic curvature χ^{nel} is assumed to vanish, so that, by virtue Eq.(1), total and elastic curvatures are coincident $\chi = \chi^{el}$.

Cantilever under concentrated couple at free end.

Let us consider a cantilever of length L and uniform bending stiffness K under a concentrated couple \mathcal{M} applied at free end.

The bending moment field M is obtained by the differential equilibrium equation $\partial_x^2 M = 0$ equipped with standard natural boundary conditions $M(L) = \mathcal{M}$ and $\partial_x M(L) = 0$, so that Eq.(11) becomes

$$\frac{\mathcal{M}}{c^2} = \frac{K\chi^{el}(x)}{c^2} - \alpha K\partial_x^2\chi^{el}(x) \quad (16)$$

supplemented with the constitutive boundary conditions

$$\begin{cases} -\mathcal{M} = \alpha K \left(c\partial_x\chi^{el}(0) - \chi^{el}(0) \right) \\ \mathcal{M} = \alpha K \left(c\partial_x\chi^{el}(L) + \chi^{el}(L) \right) \end{cases} \quad (17)$$

Solving the differential problem in Eqs.(16)-(17) provides the elastic curvature χ^{el} . Also, Eq.(1) with prescription of standard essential boundary conditions $v(0) = 0$ and $\partial_x v(0) = 0$, gives the nonlocal displacement field

$$v(x) = \frac{\mathcal{M}x^2}{2K} - \frac{\mathcal{M}}{\psi_1 K} c(\alpha - 1) e^{-\frac{x}{c\sqrt{\alpha}}} \left((x - c\sqrt{\alpha}) e^{\frac{L+x}{c\sqrt{\alpha}}} + c\sqrt{\alpha} e^{\frac{L}{c\sqrt{\alpha}}} - e^{\frac{x}{c\sqrt{\alpha}}} (c\sqrt{\alpha} + x) + c\sqrt{\alpha} e^{\frac{2x}{c\sqrt{\alpha}}} \right) \quad (18)$$

with

$$\psi_1 = (\sqrt{\alpha} + 1) e^{\frac{L}{c\sqrt{\alpha}}} + \sqrt{\alpha} - 1 \quad (19)$$

Cantilever under concentrated force at free end.

Let us consider a cantilever of length L and uniform bending stiffness K under a concentrated force F applied at free end.

The equilibrated bending moment field M is defined by $\partial_x^2 M = 0$ with prescription of standard natural boundary conditions $M(L) = 0$ and $\partial_x M(L) = -F$, so that Eq.(11) becomes

$$\frac{F(L-x)}{c^2} = \frac{K\chi^{el}(x)}{c^2} - \alpha K \partial_x^2 \chi^{el}(x) \quad (20)$$

equipped with the constitutive boundary conditions

$$\begin{cases} -Fc - FL = \alpha K \left(c \partial_x \chi^{el}(0) - \chi^{el}(0) \right) \\ -Fc = \alpha K \left(c \partial_x \chi^{el}(L) + \chi^{el}(L) \right) \end{cases} \quad (21)$$

The unknown elastic curvature χ^{el} is obtained by solving the differential problem in Eqs.(20)-(21). Then, Eq.(1) with prescription of standard essential boundary conditions provides the following nonlocal displacement field

$$v(x) = \frac{Fx^2(3L-x)}{6K} + \frac{(\alpha-1)cF}{\psi K} e^{-\frac{x}{\sqrt{\alpha}c}} \left(\sqrt{\alpha} \psi_1 c^2 (e^{\frac{x}{\sqrt{\alpha}c}} - 1) (e^{\frac{L}{\sqrt{\alpha}c}} + e^{\frac{x}{\sqrt{\alpha}c}}) - \psi_2 L x e^{\frac{x}{\sqrt{\alpha}c}} + \psi_3 c \right) \quad (22)$$

with

$$\begin{aligned}
\psi &= (\sqrt{\alpha} + 1)^2 e^{\frac{2L}{\sqrt{\alpha}c}} - (\sqrt{\alpha} - 1)^2 \\
\psi_2 &= \sqrt{\alpha} + (\sqrt{\alpha} + 1) e^{\frac{2L}{\sqrt{\alpha}c}} - 1 \\
\psi_3 &= -(\sqrt{\alpha} + 1) \sqrt{\alpha} L e^{\frac{2L}{\sqrt{\alpha}c}} + (\alpha - \sqrt{\alpha}) L e^{\frac{2x}{\sqrt{\alpha}c}} - 2\sqrt{\alpha} x e^{\frac{L+x}{\sqrt{\alpha}c}} + \\
&(\sqrt{\alpha} + 1)(\sqrt{\alpha}L - x) e^{\frac{2L+x}{\sqrt{\alpha}c}} - (\sqrt{\alpha} - 1) e^{\frac{x}{\sqrt{\alpha}c}} (\sqrt{\alpha}L + x)
\end{aligned} \tag{23}$$

Simply supported beam under uniformly distributed loading.

Let us consider a simply supported beam of length L and uniform bending stiffness K under uniformly distributed loading q .

Bending moment field M is determined by differential equilibrium equation $\partial_x^2 M = q$ equipped with natural boundary conditions $M(0) = 0$ and $M(L) = 0$, so that Eq.(11) becomes

$$\frac{qx(x-L)}{2c^2} - q = \frac{K\chi^{el}}{c^2} - \alpha K \partial_x^2 \chi^{el} \tag{24}$$

supplemented with constitutive boundary conditions

$$\begin{cases} -c \frac{qL}{2} = \alpha K \left(c \partial_x \chi^{el}(0) - \chi^{el}(0) \right) \\ c \frac{qL}{2} = \alpha K \left(c \partial_x \chi^{el}(L) + \chi^{el}(L) \right) \end{cases} \tag{25}$$

The elastic curvature χ^{el} is obtained from Eqs.(24)-(25); then, Eq.(1) together with essential boundary conditions $v(0) = 0$ and $v(L) = 0$, provides the nonlocal displacement field

$$\begin{aligned}
v(x) &= \frac{qx(L^3 - 2Lx^2 + x^3)}{24K} - \frac{(\alpha - 1)c^2 q}{2\psi_1 K} e^{-\frac{x}{\sqrt{\alpha}c}} \left(-e^{\frac{x}{\sqrt{\alpha}c}} (2\alpha^{3/2} c^2 + L(\sqrt{\alpha}c \right. \\
&- \sqrt{\alpha}x + x) + (\sqrt{\alpha} - 1)x^2) + e^{\frac{L+x}{\sqrt{\alpha}c}} (-2\alpha^{3/2} c^2 + L(-\sqrt{\alpha}c + \sqrt{\alpha}x \\
&+ x) - (\sqrt{\alpha} + 1)x^2) + \sqrt{\alpha} c e^{\frac{L}{\sqrt{\alpha}c}} (2\alpha c + L) + \sqrt{\alpha} c (2\alpha c + L) e^{\frac{2x}{\sqrt{\alpha}c}} \end{aligned} \tag{26}$$

Doubly clamped beam under uniformly distributed loading.

Let us consider a doubly clamped beam of length L and uniform bending stiffness K under uniformly distributed loading q .

The bending moment field M obtained by the differential equilibrium equation $\partial_x^2 M = q$ is a function of two integration constants, a_1 and a_2 . Hence, Eq.(11) in terms of displacement field v becomes

$$\frac{qx^2}{2} + a_1x + a_2 - c^2q = K\partial_x^2v - \alpha c^2 K\partial_x^4v \quad (27)$$

supplemented with constitutive and kinematic boundary conditions

$$\left\{ \begin{array}{l} ca_1 - a_2 = \alpha K (c\partial_x^3v(0) - \partial_x^2v(0)) \\ c(qL + a_1) + \frac{qL^2}{2} + a_1L + a_2 = \alpha K (c\partial_x^3v(L) + \partial_x^2v(L)) \\ v(0) = 0 \\ \partial_xv(0) = 0 \\ v(L) = 0 \\ \partial_xv(L) = 0 \end{array} \right. \quad (28)$$

By solving the differential problem in Eqs.(27)-(28) the nonlocal displacement field is given by

$$\begin{aligned} v(x) = & \frac{qx^2(L-x)^2}{24K} + \frac{c(\alpha-1)q}{12\psi_4K}(12c^2 + 6cL + L^2)e^{-\frac{x}{\sqrt{\alpha c}}}(\sqrt{\alpha}cLe^{\frac{L}{\sqrt{\alpha c}}} \\ & - e^{\frac{L+x}{\sqrt{\alpha c}}}(\sqrt{\alpha}cL - Lx + x^2) + e^{\frac{x}{\sqrt{\alpha c}}}(-\sqrt{\alpha}cL - Lx + x^2) + \sqrt{\alpha}cLe^{\frac{2x}{\sqrt{\alpha c}}}) \end{aligned} \quad (29)$$

with

$$\psi_4 = L(-\sqrt{\alpha} - (\sqrt{\alpha} + 1)e^{\frac{L}{\sqrt{\alpha c}}} + 1) + 2(\alpha - 1)c(e^{\frac{L}{\sqrt{\alpha c}}} - 1) \quad (30)$$

5. Inconsistency of limiting solutions

As enlightened by theoretical outcomes in Sect.3, no solution can be found to Eq.(3) for a vanishing mixture parameter, i.e.: $\alpha = 0$. Indeed, for any value $c > 0$, constitutive boundary conditions in Eq.(12) can be satisfied by equilibrated bending moments only for a strictly positive mixture parameter. Hence, inconsistencies of two-phase solutions are expected to occur as $\alpha \rightarrow 0$.

In the following, analytical limiting responses of case-studies in Sec.4 are provided. Non-dimensional variables are used in parametric plots by introducing the non-dimensional abscissa $\xi = x/L$, the nonlocal parameter $\lambda = c/L$ and the following non-dimensional limiting displacement fields

$$\bar{v}_l = v_l \frac{K}{FL^3} \quad \text{or} \quad \bar{v}_l = v_l \frac{K}{\mathcal{M}L^2} \quad \text{or} \quad \bar{v}_l = v_l \frac{K}{qL^4} \quad (31)$$

Cantilever under concentrated couple at free end.

Computing the limit as $\alpha \rightarrow 0$ of Eq.(18), we get the following limiting displacement field

$$v_l(x) = \frac{\mathcal{M}}{K} \left(\frac{x^2}{2} + cx \right) \quad (32)$$

The displacement field in Eq.(32) is clearly in contrast with essential boundary conditions prescribed by constraints. Indeed, except for the local case $\lambda = 0^+$, kinematic inconsistency is apparent in parametric plots of displacement (Fig.1) and rotation fields (Fig.2) obtained from derivation of Eq.(32).

Double derivation of Eq.(32) leads to the limiting elastic bending curvature χ_l that inserted into the integral convolution in Eq.(3) (with $\alpha = 0$) should provide the equilibrated bending moment. Moreover, since the redundancy degree is zero, equilibrated bending interaction is the uniform field univocally determined by equilibrium conditions. As clearly shown by parametric plots in Fig.3, the limiting elastic nonlocal curvature χ_l provides a bending moment which is not equilibrated; indeed, it is not uniform and not equal to the applied couple, except for the asymptotic local bending moment which is equilibrated for $\xi \in]0, 1[$. A further derivation leads to shear force field which is not vanishing (see Fig.4), except for $\lambda = 0^+$ with $\xi \in]0, 1[$.

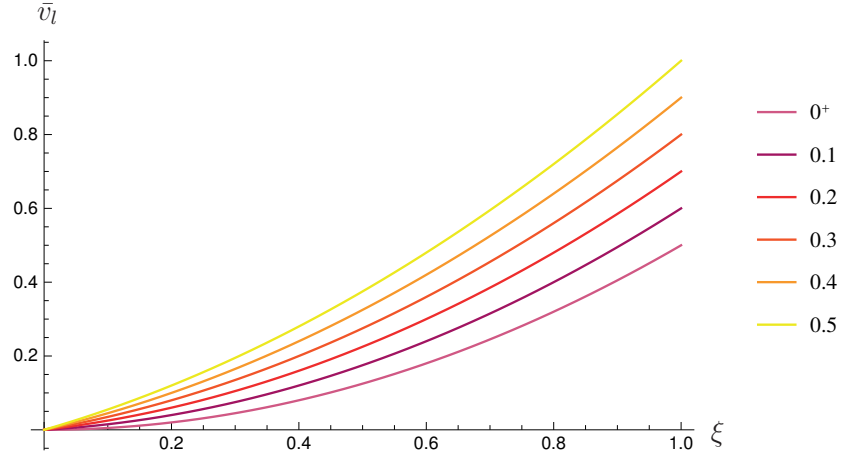


Figure 1: Cantilever under concentrated couple at free end: displacement \bar{v}_l versus ξ for $\lambda \in \{0^+, 0.1, 0.2, 0.3, 0.4, 0.5\}$.

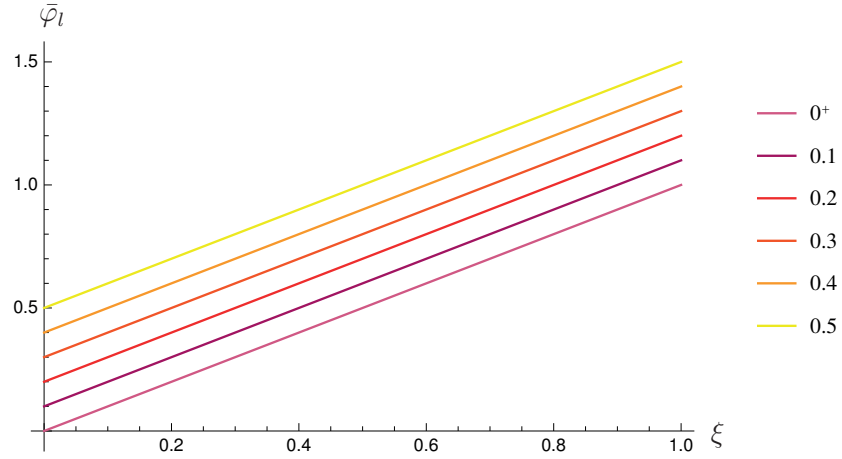


Figure 2: Cantilever under concentrated couple at free end: rotation $\bar{\varphi}_l$ versus ξ for $\lambda \in \{0^+, 0.1, 0.2, 0.3, 0.4, 0.5\}$.

Cantilever under concentrated force at free end.

Computing the limit as $\alpha \rightarrow 0$ of Eq.(22), we get the following limiting displacement field

$$v_l(x) = \frac{F}{K} \left(L \frac{x^2}{2} - \frac{x^3}{6} + c^2 x + L c x \right) \quad (33)$$

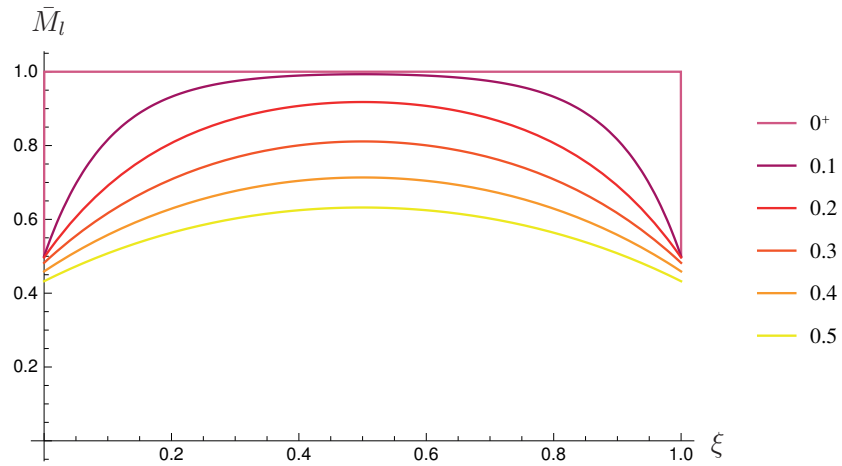


Figure 3: Cantilever under concentrated couple at free end: bending moment \bar{M}_l versus ξ for $\lambda \in \{0^+, 0.1, 0.2, 0.3, 0.4, 0.5\}$.

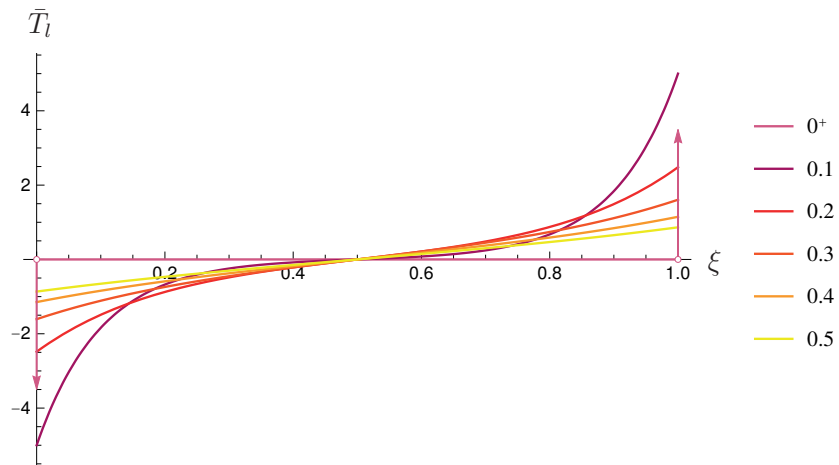


Figure 4: Cantilever under concentrated couple at free end: shear force \bar{T}_l versus ξ for $\lambda \in \{0^+, 0.1, 0.2, 0.3, 0.4, 0.5\}$.

Kinematic inconsistencies are clearly shown in parametric plots of displacement and rotation fields as a function of λ , except for the local case $\lambda = 0^+$ (see Figs.5-6). Double derivation of Eq.(33) leads to the limiting bending curvature that inserted into the integral convolution in Eq.(3), for $\alpha = 0$, provides a bending moment field which is not compatible with differential and boundary equilibrium requirements.

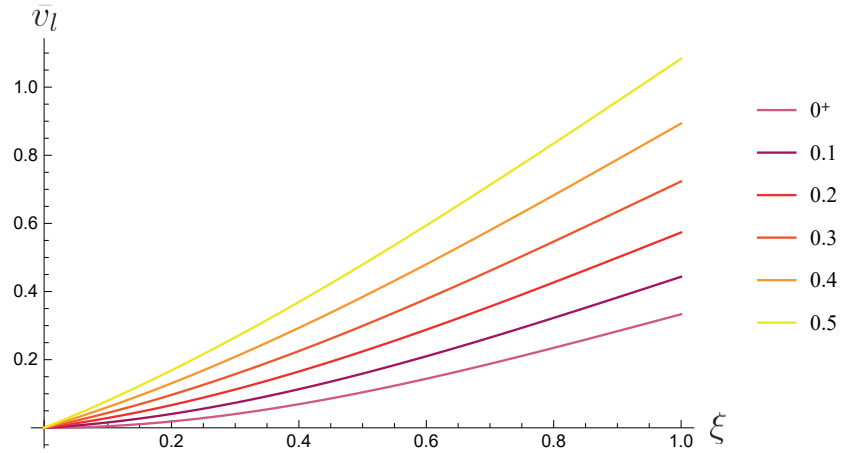


Figure 5: Cantilever under concentrated force at free end: displacement \bar{v}_l versus ξ for $\lambda \in \{0^+, 0.1, 0.2, 0.3, 0.4, 0.5\}$.

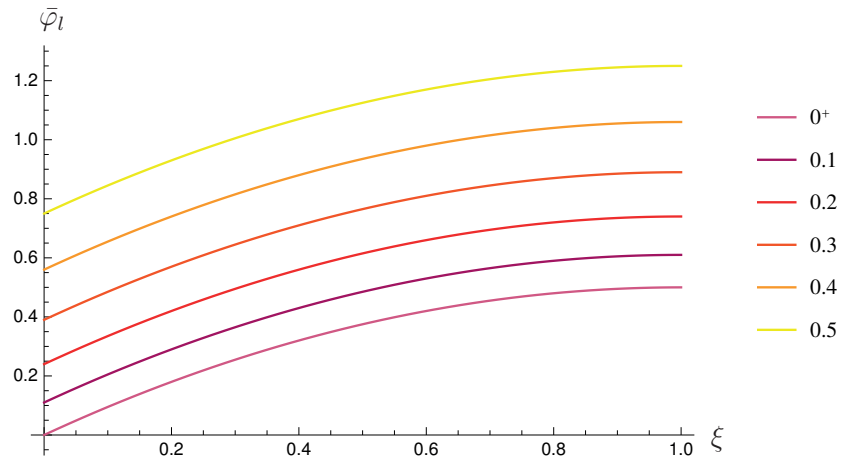


Figure 6: Cantilever under concentrated force at free end: rotation $\bar{\varphi}_l$ versus ξ for $\lambda \in \{0^+, 0.1, 0.2, 0.3, 0.4, 0.5\}$.

Indeed, since the redundancy degree is zero, the equilibrated bending moment is the linear field univocally determined by equilibrium conditions. Instead, as clearly shown by parametric plots in Fig.7, the limiting elastic bending curvature χ_l provides a bending moment which is not equilibrated since it is not linear and does not vanish at free-end of the cantilever, except for the asymptotic local bending moment which is equilibrated for $\xi \in]0, 1]$.

A further derivation leads to the shear force field which is not equal to the value of the applied force (see Fig.8) and hence, it is not uniform (except for $\lambda = 0^+$ with $\xi \in]0, 1[$), i.e.: the emerging distributed loading is not vanishing.

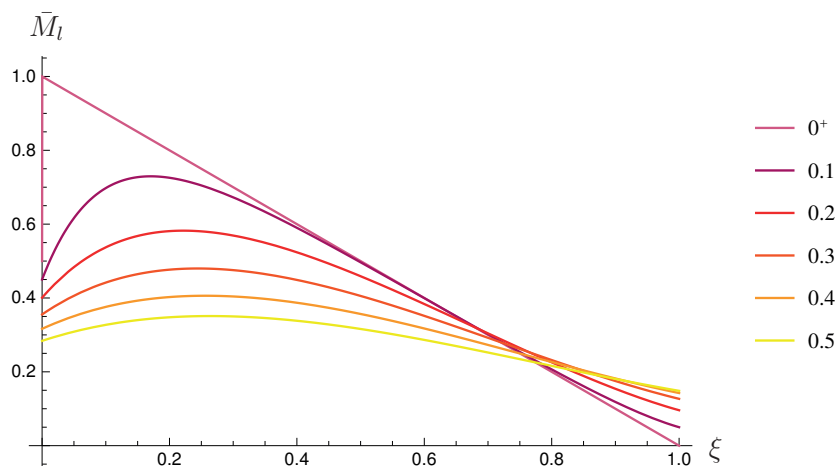


Figure 7: Cantilever under concentrated force at free end: bending moment \bar{M}_l versus ξ for $\lambda \in \{0^+, 0.1, 0.2, 0.3, 0.4, 0.5\}$.

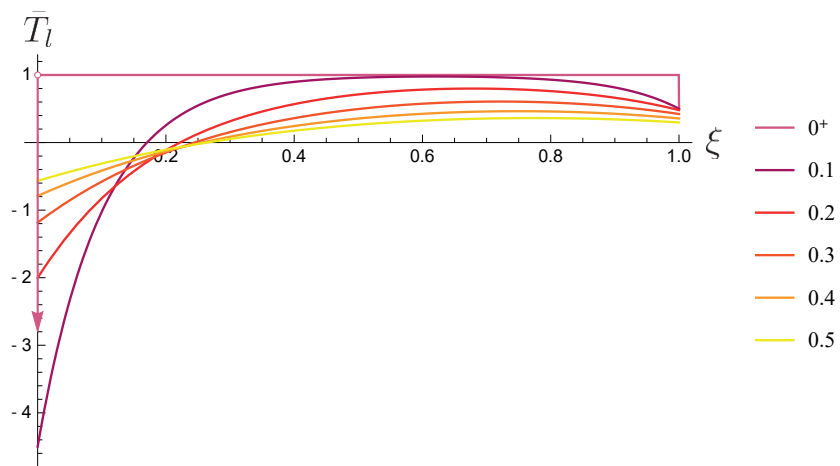


Figure 8: Cantilever under concentrated force at free end: shear force \bar{T}_l versus ξ for $\lambda \in \{0^+, 0.1, 0.2, 0.3, 0.4, 0.5\}$.

Simply supported beam under uniformly distributed loading.

Computing the limit as $\alpha \rightarrow 0$ of Eq.(26), we get the following limiting displacement

$$v_l(x) = \frac{q}{K} \left(\frac{x^4}{24} - \frac{Lx^3}{12} - \frac{c^2x^2}{2} + \frac{L^3x}{24}(12\lambda^2 + 1) \right) \quad (34)$$

Parametric plots of displacement and rotation fields as function of λ are shown in Figs.9-10. Double derivation of Eq.(34) leads to the limiting bending curvature that inserted into the integral convolution in Eq.(3) (for $\alpha = 0$) provides the static fields shown in Figs.11-12. The bending moment field is clearly incompatible with natural boundary conditions and the shear force field is not linear, i.e.: the emerging distributed loading is not uniform (see Fig.13). Hence, the interaction fields for $\lambda > 0$ are not compatible with differential and boundary equilibrium requirements.

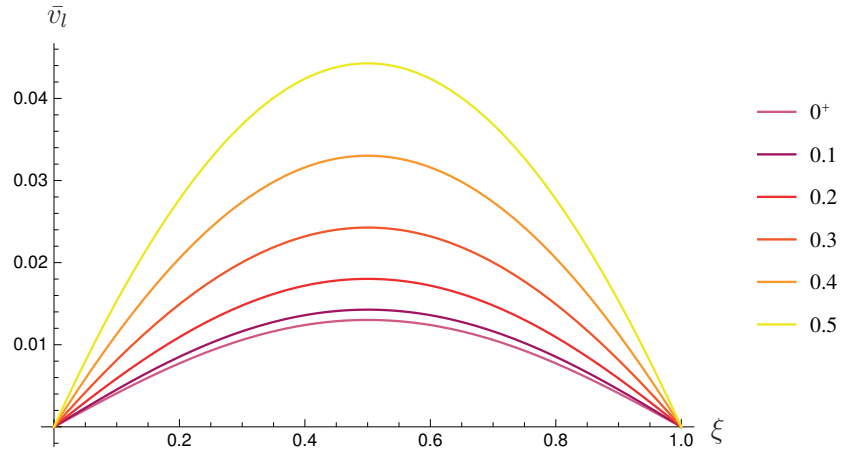


Figure 9: Simply supported beam under uniformly distributed loading: displacement \bar{v}_l versus ξ for $\lambda \in \{0^+, 0.1, 0.2, 0.3, 0.4, 0.5\}$.

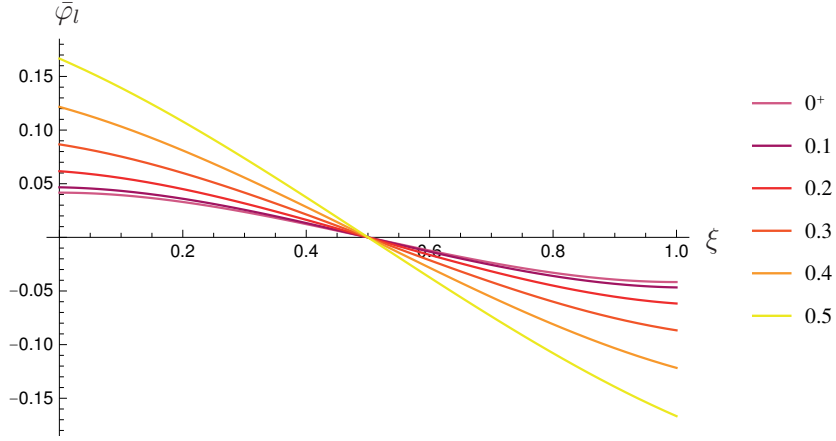


Figure 10: Simply supported beam under uniformly distributed loading: rotation $\bar{\varphi}_l$ versus ξ for $\lambda \in \{0^+, 0.1, 0.2, 0.3, 0.4, 0.5\}$.

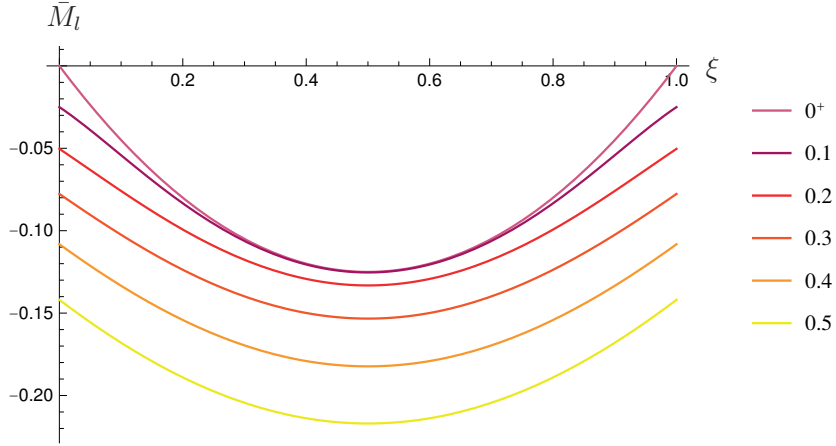


Figure 11: Simply supported beam under uniformly distributed loading: bending moment \bar{M}_l versus ξ for $\lambda \in \{0^+, 0.1, 0.2, 0.3, 0.4, 0.5\}$.

Doubly clamped beam under uniformly distributed loading.

The limiting displacement field as $\alpha \rightarrow 0$ of Eq.(29) is given by

$$v_l(x) = \frac{q}{K} \left(\frac{x^4}{24} - \frac{Lx^3}{12} - \frac{c^2x^2}{2} + \frac{c(12\lambda^2 + 6\lambda + 1)L^2x}{12(2\lambda + 1)} + \frac{L^2x^2}{24(2\lambda + 1)} \right) \quad (35)$$

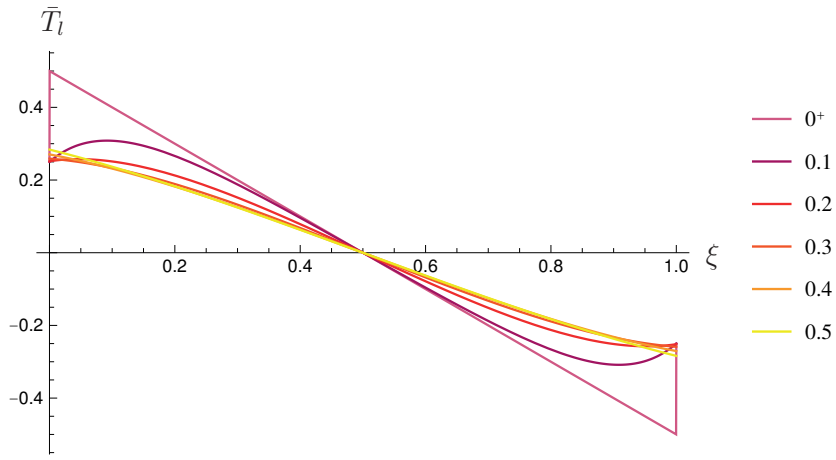


Figure 12: Simply supported beam under uniformly distributed loading: shear force \bar{T}_l versus ξ for $\lambda \in \{0^+, 0.1, 0.2, 0.3, 0.4, 0.5\}$.

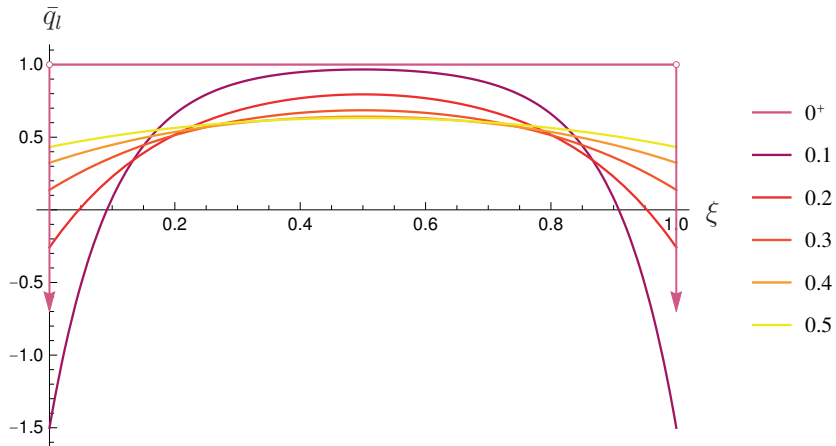


Figure 13: Simply supported beam under uniformly distributed loading: emerging loading \bar{q}_l versus ξ for $\lambda \in \{0^+, 0.1, 0.2, 0.3, 0.4, 0.5\}$.

The displacement field in Eq.(35) is in contrast with essential boundary conditions prescribed by constraints. These kinematic inconsistencies are clearly shown in parametric plots of displacement and rotation fields (see Figs.14-15). Double derivation of Eq.(33) leads to the limiting nonlocal elastic curvature that is used to compute the integral convolution in Eq.(3), for $\alpha = 0$, to get the bending moment field depicted in Fig.16. A further derivation leads to shear force field which is not linear (see Fig.17) and the

emerging distributed loading is not uniform and not equal to the applied one (see Fig.18). Hence, limiting solutions of the elastostatic problem do not satisfy kinematic compatibility and equilibrium requirements, except for the asymptotic local displacement and rotation fields $\forall \xi \in [0, 1]$ and for the asymptotic local bending and shearing fields for $\xi \in]0, 1[$.

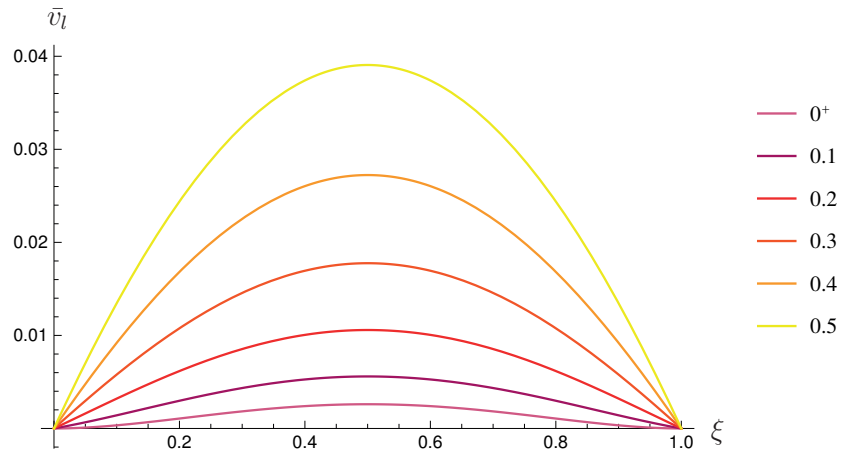


Figure 14: Doubly clamped beam under uniformly distributed loading: displacement \bar{v}_l versus ξ for $\lambda \in \{0^+, 0.1, 0.2, 0.3, 0.4, 0.5\}$.

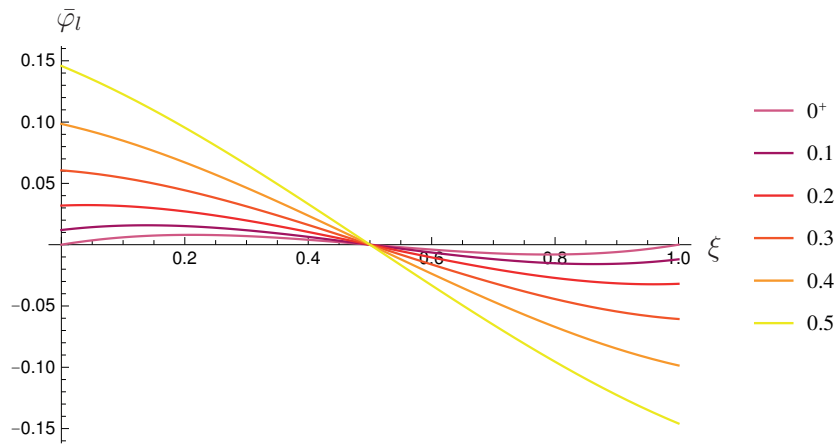


Figure 15: Doubly clamped beam under uniformly distributed loading: rotation $\bar{\varphi}_l$ versus ξ for $\lambda \in \{0^+, 0.1, 0.2, 0.3, 0.4, 0.5\}$.

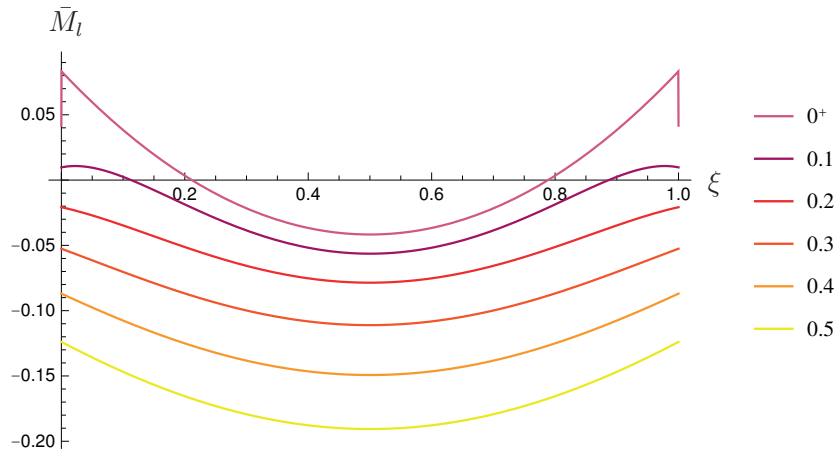


Figure 16: Doubly clamped beam under uniformly distributed loading: bending moment \bar{M}_l versus ξ for $\lambda \in \{0^+, 0.1, 0.2, 0.3, 0.4, 0.5\}$.

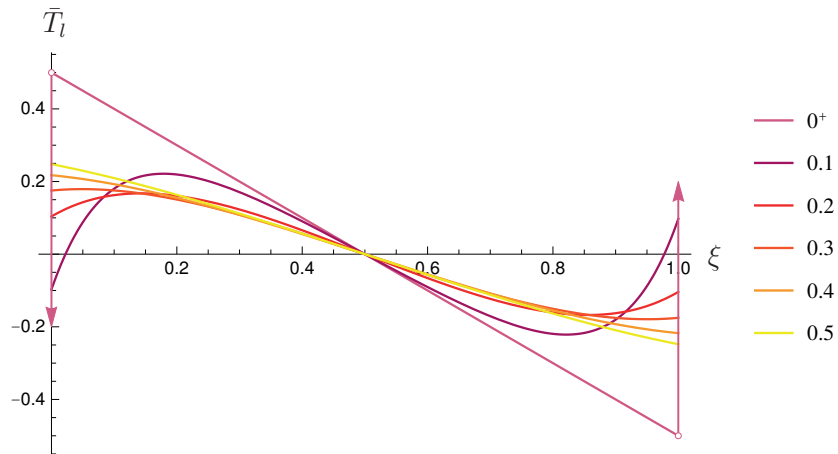


Figure 17: Doubly clamped beam under uniformly distributed loading: shear force \bar{T}_l versus ξ for $\lambda \in \{0^+, 0.1, 0.2, 0.3, 0.4, 0.5\}$.

6. Closing remarks

The bending behaviour of elastic beams has been investigated by Eringen's two-phase integral theory. Exact closed-form solutions of simple structural problems of applicative interest have been preliminarily provided in terms of mixture and nonlocal parameters. Then, relevant asymptotic fields (as the mixture parameter tends to zero) have been evaluated and studied.

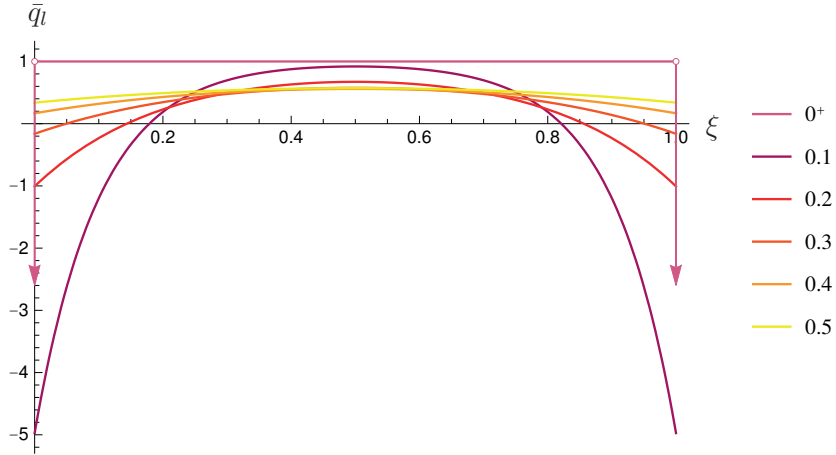


Figure 18: Doubly clamped beam under uniformly distributed loading: emerging loading \bar{q}_l versus ξ for $\lambda \in \{0^+, 0.1, 0.2, 0.3, 0.4, 0.5\}$.

It has been proven that such fields are in contrast with kinematic boundary conditions and equilibrium requirements for any nonlocal parameter value. Accordingly, limiting responses of Eringen's two-phase formulation cannot be used as solutions of the ill-posed Eringen purely nonlocal structural problem. Therefore, inaccurate outcomes contributed in current literature (see e.g. [Mikhasev and Nobili, 2020](#); [Mikhasev, 2021](#)), regarding the well-posedness of limiting elastodynamic problems based on Eringen's two-phase continuum theory, should be amended consequently.

Acknowledgment - Financial support from the MIUR in the framework of the Project PRIN 2017 - code 2017J4EAYB *Multiscale Innovative Materials and Structures (MIMS)*; University of Naples Federico II Research Unit - is gratefully acknowledged.

References

- Banejad, A., Passandideh-Fard, M., Niknam, H., Mirshojaeian Hosseini, M.J., Mousavi Shaegh, S.A., 2020. Design, fabrication and experimental characterization of whole-thermoplastic microvalves and micropumps having micromilled liquid channels of rectangular and half-elliptical cross-sections. *Sensors and Actuators A* 301, 111713.
- Barretta, R., Fabbrocino, F., Luciano, R., Marotti de Sciarra, F., 2018a. Closed-form solutions in stress-driven two-phase integral elasticity for bending of functionally graded nano-beams. *Physica E: Low-dimensional Systems and Nanostructures* 97, 13–30.
- Barretta, R., Čanadija, M., Feo, L., Luciano, R., Marotti de Sciarra, F., Penna, R., 2018b. Exact solutions of inflected functionally graded nano-beams in integral elasticity. *Composites Part B* 142, 273-286.
- Barretta, R., Diaco, M., Feo, L., Luciano, R., Marotti de Sciarra, F., Penna, R., 2018c. Stress-driven integral elastic theory for torsion of nano-beams. *Mechanics Research Communications* 87, 35-41.
- Barretta, R., Marotti de Sciarra, F., Vaccaro, M.S., 2019. On nonlocal mechanics of curved elastic beams. *International Journal of Engineering Science* 144, 103140.
- Bažant, Z.P., Jirásek, M., 2002. Nonlocal integral formulation of plasticity and damage: survey of progress. *Journal of Engineering Mechanics - ASCE*, 128, 1119-1149.
- Borino, G., Failla, B., Parrinello, F., 2003. A symmetric nonlocal damage theory. *International Journal of Solids and Structures* 40, 3621-3645.
- Chao, M., Wang, Y., Ma, D., Wu, X., Zhang, W., Zhang, L., Wan, P., 2020. Wearable mxene nanocomposites-based strain sensor with tile-like stacked hierarchical microstructure for broad-range ultrasensitive sensing. *Nano Energy* 78, 105187.
- Chorsi, M.T. , Chorsi, H.T., 2018. Modeling and analysis of MEMS disk resonators. *Microsystem Technologies* 24 (6), 2517–2528 .
- Eringen, A. C., 1972. Linear theory of nonlocal elasticity and dispersion of plane waves. *International Journal of Engineering Science* 10(5), 425-435.

- Eringen, A. C., 1983. On differential equations of nonlocal elasticity and solutions of screw dislocation and surface waves. *Journal of Applied Physics* 54, 4703.
- Eringen, A. C., 1987. Theory of nonlocal elasticity and some applications. *Res Mechanica* 21, 313-342.
- Eptaimeros, K.G., Koutsoumaris, C.C., Tsamasphyros, G.J., 2016. Nonlocal integral approach to the dynamical response of nano-beams. *Int J Mech Sci* 115–116, 68–80 .
- Fathi, M., Ghassemi, A. (2017). The effects of surface stress and nonlocal small scale on the uniaxial and biaxial buckling of the rectangular piezo-electric nanoplate based on the two variable-refined plate theory. *Journal of the Brazilian Society of Mechanical Sciences and Engineering* 39 3203-3216.
- Fernández-Sáez, J., Zaera, R., 2017. Vibrations of Bernoulli-Euler beams using the two-phase nonlocal elasticity theory. *International Journal of Engineering Science* 119, 232-248.
- Ghayesh, M.H., Farajpour, A., 2019. A review on the mechanics of functionally graded nanoscale and microscale structures. *International Journal of Engineering Science* 137, 8-36.
- Ghayesh, M.H., Farokhi, H., 2020. Nonlinear broadband performance of energy harvesters. *Int J Eng Sci* 147, 103202
- Jankowski, P., Żur, K.K., Kim, J., Reddy, J.N., 2020. On the bifurcation buckling and vibration of porous nanobeams. *Composite Structures* 250, 112632.
- Karami, B., Shahsavari, D., Janghorban, M., Li, L., 2018. Wave dispersion of mounted graphene with initial stress. *Thin-Walled Structures* 122, 102-111.
- Kiani, K., Żur, K.K., 2021. Vibrations of double-nanorod-systems with defects using nonlocal-integralsurface energy-based formulations. *Composite Structures* 256, 113028.
- Khodabakhshi, P., Reddy, J.N., 2015. A unified integro-differential nonlocal model. *International Journal of Engineering Science* 95, 60-75.

- Kröner, E., 1967. Elasticity theory of materials with long range cohesive forces. *International Journal of Solids and Structures* 3(5), 731-742.
- Lu, P., Veletić, M., Laasmaa, M., Vendelin, M., Louch, W.E., Steinar Halvorsen P., Bergsland, J., Balasingham, I., 2019. Multi-nodal nano-actuator pacemaker for energy-efficient stimulation of cardiomyocytes. *Nano Communication Networks* 22, 100270.
- Malikan, M., Eremeyev, V.A., Žur, K.K., 2020. Effect of axial porosities on flexomagnetic response of in-plane compressed piezomagnetic nanobeams. *Symmetry* 12(12), 1935.
- Mikhasev, G., Nobili, A., 2020. On the solution of the purely nonlocal theory of beam elasticity as a limiting case of the two-phase theory. *International Journal of Solids and Structures* 190, 47–57.
- Mikhasev, G., 2021. Free high-frequency vibrations of nonlocally elastic beam with varying cross-section area. *Continuum Mechanics and Thermodynamics*. <https://doi.org/10.1007/s00161-021-00977-6>
- Oskouie, M. F., Ansari, R., Rouhi, H., 2018. Bending of Euler-Bernoulli nanobeams based on the strain-driven and stress-driven nonlocal integral models: a numerical approach. *Acta Mechanica Sinica*. Doi: 10.1007/s10409-018-0757-0
- Pinnola, F.P., Vaccaro, M.S., Barretta, R., Marotti de Sciarra, F., 2020. Random vibrations of stress-driven nonlocal beams with external damping. *Meccanica* URL <https://doi.org/10.1007/s11012-020-01181-7>.
- Pisano, A.A., Fuschi, P., 2003. Closed form solution for a nonlocal elastic bar in tension. *International Journal of Solids and Structures* 40, 13-23.
- Pisano, A.A., Fuschi, P., Polizzotto, C., 2021. Integral and differential approaches to Eringen's nonlocal elasticity models accounting for boundary effects with applications to beams in bending. *ZAMM - Journal of Applied Mathematics and Mechanics*. <https://doi.org/10.1002/zamm.202000152>
- Polizzotto, C., 2001. Nonlocal elasticity and related variational principles. *International Journal of Solids and Structures* 38, 7359-7380.

- Polizzotto, C., 2002. Thermodynamics and continuum fracture mechanics for nonlocal-elastic plastic materials. *European Journal of Mechanics A/Solids* 21, 85-103.
- Polyanin, A.D., Manzhirov A.V., 2008. Handbook of integral equations. 2nd ed. Boca Raton, FL: Chapman & Hall/CRC.
- Roghani, M., Rouhi, H., 2020. Nonlinear stress-driven nonlocal formulation of timoshenko beams made of fgms. *Continuum Mechanics and Thermodynamics*. <https://doi.org/10.1007/s00161-020-00906-z>
- Rogula, D., 1965. Influence of spatial acoustic dispersion on dynamical properties of dislocations. *Bulletin de l'Académie Polonaise des Sciences, Séries des Sciences Techniques* 13, 337-343 .
- Rogula, D., 1982. Introduction to nonlocal theory of material media. In D. Rogula (Ed.), *Nonlocal theory of material media*, CISM courses and lectures (vol. 268, pp. 125-222). Wien: Springer.
- Romano, G., Barretta, R., Diaco, M., Marotti de Sciarra, F., 2017a. Constitutive boundary conditions and paradoxes in nonlocal elastic nano-beams. *International Journal of Mechanical Sciences* 121, 151-156.
- Romano, G., Barretta, R., Diaco, M., 2017b. On nonlocal integral models for elastic nano-beams. *International Journal of Mechanical Sciences* 131-132, 490-499.
- Sedighi, H.M., Malikan, M., Valipour, A., Żur, K.K., 2020. Nonlocal vibration of carbon/boron-nitride nano-hetero-structure in thermal and magnetic fields by means of nonlinear finite element method. *Journal of Computational Design and Engineering* 7(5), 591-602.
- Soukarié, D., Ecochard, V., Salomé, L., 2020. Dna-based nanobiosensors for monitoring of water quality. *Int. J. Hyg. Environ. Health* 226, 113485.
- Tricomi, F.G., 1957. *Integral Equations*. Interscience, New-York, USA. Reprinted by Dover Books on Mathematics, 1985.
- Vila, J., Fernández-Sáez, J., Zaera, R., 2017. Nonlinear continuum models for the dynamic behavior of 1D microstructured solids. *International Journal of Solids and Structures* 117, 111-122.

- Wang, Y., Zhu, X., Dai, H., 2016. Exact solutions for the static bending of Euler-Bernoulli beams using Eringen two-phase local/nonlocal model. *AIP Advances* 6(8), 085114. Doi:10.1063/1.4961695
- Zhang, Y., 2017. Frequency spectra of nonlocal Timoshenko beams and an effective method of determining nonlocal effect. *International Journal of Mechanical Sciences* 128-129, 572-582.
- Zhang, J.Q., Qing, H., Gao, C.F., 2020. Exact and asymptotic bending analysis of microbeams under different boundary conditions using stress-derived nonlocal integral model. *Z. Angew. Math. Mech.* 100(1), e201900148.
- Zhu, X., Li, L., 2017. Closed form solution for a nonlocal strain gradient rod in tension. *International Journal of Engineering Science* 119, 16-28.
- Zur, K.K., Arefi, M., Kimc, J., Reddy, J.N., 2020. Free vibration and buckling analyses of magneto-electro-elastic FGM nanoplates based on nonlocal modified higher-order sinusoidal shear deformation theory. *Composites Part B* 182, 107601.